Chapter 37
Contour Method Residual Stress Measurement Uncertainty in a Quenched Aluminum Bar and a Stainless Steel Welded Plate

Mitchell D. Olson, Adrian T. DeWald, Michael B. Prime, and Michael R. Hill

Abstract This paper describes a newly developed uncertainty estimate for contour method residual stress measurements and presents results from two experiments where the uncertainty estimate was applied. The uncertainty estimate includes contributions from random error sources including the error arising from noise in displacement measurements and the smoothing of the displacement surfaces. The output is a two-dimensional, spatially varying uncertainty estimate such that every point on the cross-section where residual stress is determined has a corresponding uncertainty value. The current paper describes the use of the newly developed uncertainty estimate in a quenched aluminum bar with a cross section of 51 × 76 mm and a stainless steel weld plate with a cross-section of 25.4 × 152.4 mm, with a 6.35 mm deep groove, filled with a multi-pass weld. The estimated uncertainty in the quenched aluminum bar is approximately 5 MPa over the majority of the cross-section, with localized areas of higher uncertainty, up to 10 MPa. The estimated uncertainty in the welded stainless steel plate is approximately 22 MPa over the majority of the cross-section, with localized areas of higher uncertainty, over 50 MPa.

Keywords Residual stress measurement • Contour method • Uncertainty quantification • Repeatability • Aluminum alloy 7050-T74 • Quenching

37.1 Introduction

The contour method is a residual stress measurement technique that is capable of generating a two-dimensional map of residual stress over a plane in a body. The theoretical underpinning of the method is given by Prime [1], and is based on the fact that when a residual stress bearing body is cut in half, stresses are released and redistributed within the body, which causes deformation. The out-of-plane displacements are directly related to the stresses released, and the technique comprises measurement of the out-of-plane displacements at the cut plane and use of the measured displacements to determine residual stress at the cut plane via elastic stress analysis (Fig. 37.1). The contour method has been used to measure residual stress for a variety of conditions [2–5].

Currently, only limited work has been performed for uncertainty estimation of the contour method. Some researchers have used an *overall* uncertainty estimate (e.g., a single uncertainty value for every measured point on the cross-section) based on the noise present in the surface topography data [6, 7] and measuring the surface topography with different instruments [8]. Another study found the uncertainty using differences in residual stress from different levels of smoothing [9], but required that the surface use a similar level of smoothing in both spatial directions. The newly developed uncertainty estimate [10] is the first to develop a single measurement uncertainty estimator for the contour method, where the estimated uncertainty is a function of in-plane position and is applicable for arbitrary surface smoothing, and to show the uncertainty

M.D. Olson (✉)
Hill Engineering, LLC, 3035 Prospect Park Drive Suite 180, Rancho Cordova, CA 95670, USA

Department of Mechanical and Aerospace Engineering, University of California, One Shields Avenue, Davis, CA 95616, USA
e-mail: molson@ucdavis.edu

A.T. DeWald
Hill Engineering, LLC, 3035 Prospect Park Drive Suite 180, Rancho Cordova, CA 95670, USA

M.B. Prime
Los Alamos National Laboratory, W-13, PO Box 1663, Los Alamos, NM 87545, USA

M.R. Hill
Department of Mechanical and Aerospace Engineering, University of California, One Shields Avenue, Davis, CA 95616, USA

S. Bossuyt et al. (eds.), *Residual Stress, Thermomechanics & Infrared Imaging, Hybrid Techniques and Inverse Problems, Volume 9*, Conference Proceedings of the Society for Experimental Mechanics Series, DOI 10.1007/978-3-319-21765-9_37

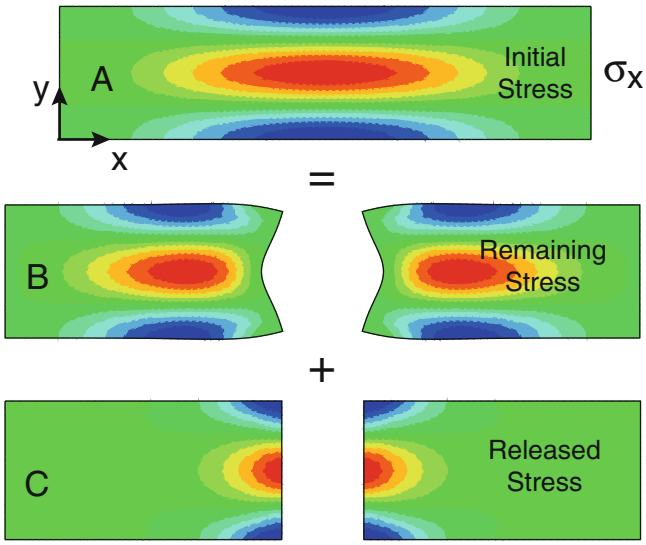

Fig. 37.1 Contour method steps: configuration A is a body containing residual stresses with the color scale corresponding to σ_{xx}; in configuration B, the body has been cut in half, creating a new stress-free surface; configuration C shows the stresses that were released in going from A to B, which can be found by reversing the cut surface deformation. Assuming elastic behavior, superposition provides A = B + C, and since σ_{xx} on the cut plane in B is zero (free surface), then σ_{xx} on the cut plane in A must be equal to σ_{xx} on the cut plane in C

estimator is a useful predictor of measurement uncertainty. The objectives of this work are to report the estimated uncertainty in two test cases using the newly developed uncertainty estimate.

37.2 Methods

The methodology for contour method uncertainty estimation is based on quantifying the uncertainty for random error sources [10]. Two random error sources identified for the contour method are the uncertainty due to noise in the displacement surfaces and the uncertainty arising from smoothing of the displacement surfaces. The uncertainty due to noise in the displacement surfaces is caused by the inherent surface roughness due to cutting, as well as the measurement error present in the displacement measurement signal. Both of these uncertainty sources show up as high frequency noise in the displacement surface, and cause what will be called the "displacement error." The other error source addressed is the uncertainty arising from the smoothing used in data processing that is required to extract the underlying form of the measured data. The amount of smoothing is selected based upon limited knowledge. Even if the optimal amount of smoothing were selected, there is no guarantee that the extracted form will exactly match the underlying trend in the displacement data. Thus, some amount of error is introduced from the data processing and this will be called the "model error." This approach for uncertainty estimation is similar to the methodology developed by Prime and Hill for uncertainty estimation in the slitting method for residual stress measurement [11].

37.2.1 Model Error

For contour method measurements, the analysis to extract the form of the experimental surface displacement (and simultaneously filter out the noise) is typically accomplished by fitting the measured surface displacements to a bivariate analytical surface. To illustrate the model error concept, consider a general bivariate, tensor product analytical surface

$$f(x,y) = \sum_{i=0}^{m} \sum_{j=0}^{n} C_{ij} P_i(x) P_j(y) \tag{37.1}$$

where x and y are spatial dimensions in the cut plane, C_{ij} are coefficients, $P_i(x)$ and $P_j(y)$ are known basis functions, and m and n are the highest order terms included in the series corresponding to the x and y spatial dimensions. The amount of smoothing is related to the choice of the fitting model (i.e., (37.1) and parameters m and n). The choice of the fitting model and parameters affects the contour method result. Earlier work on the slitting method for residual stress measurement [11] treated the smoothing model as a source of uncertainty, referred to as the "model error." Adapting that approach to the contour method, the model error is estimated by taking the standard deviation of the computed residual stresses over a range of smoothing parameters. The model error definition used is

$$U_{Model} = std(\sigma_{m,n}, \sigma_{m+1,n}, \sigma_{m,n+1}, \sigma_{m-1,n}, \sigma_{m,n-1}) \tag{37.2}$$

where U_{Model} is the model error, σ is residual stress determined by the contour method for a given smoothing model, and the subscripts refer to the amount of smoothing used in the contour data analysis. This definition of the model error includes a range of smoothing in both spatial directions and both higher and lower in spatial frequency, which provides a measure of the sensitivity of the computed residual stress to the selected fitting model. The model error is assumed to have a Gaussian distribution, which has been found to be appropriate for many experimental error sources [12], and implies that one standard deviation represents a confidence interval of 68 %.

37.2.2 Displacement Error

The contribution of the noise in the measured displacement field to the total uncertainty can be quantified using a Monte Carlo approach [13]. A statistical measure of the random noise in the experimental data is calculated from the residual of the displacement data, after the form of the surface has been extracted by fitting, where the residual is the difference between the measured surface profile and the smoothed surface profile. To estimate the influence of noise on measured residual stress, the contour method data analysis is repeated with normally distributed noise added to the measured displacements (i.e., the displacement data now contain the noise that was originally present plus random noise that was artificially introduced into the analysis). The added normally distributed noise has a standard deviation equal to the standard deviation of the residual of the displacement data. The residual stress is computed after introduction of the additional noise, and the process is repeated several times to develop a set of residual stress results, each computed with different random noise (but in every case the standard deviation of the noise is the same). The displacement error is estimated by computing the standard deviation of the set of residual stresses results with added noise, at each spatial location.

37.2.3 Total Uncertainty

The two uncertainty sources are combined together to estimate the total uncertainty. First, the root sum square of the two uncertainty sources is calculated according to

$$U_{RSS}(x,y) = \sqrt{U_{Disp}^2(x,y) + U_{Model}^2(x,y)}. \tag{37.3}$$

Next, the mean value of the root sum square uncertainty for all points on the cross-section is calculated

$$\overline{U}_{RSS} = \frac{\sum_{i=1}^{N} U_{RSS}(x_i, y_i)}{N}, \tag{37.4}$$

where (x_i, y_i) are a set of N points having roughly uniform spacing over the cross section. The pointwise measurement uncertainty is then defined as the greater of the root sum square uncertainty at each point, or the mean value

$$U_{TOT}(x, y) = \max\left(U_{RSS}(x, y), \overline{U}_{RSS}\right). \tag{37.5}$$

The inclusion of the mean value places a floor on the estimated uncertainty and ensures that it remains at a reasonable level over the entire cross section.

37.2.4 Experiments

Two contour method measurements were preformed and their associated uncertainties were estimated using the above approach. One experiment used a 7050-T74511 extruded aluminum bar that was used to confirm the usefulness of the uncertainty estimate [10] by determining the repeatability standard deviation (a measure of precision) in a set of repeat measurements (similar to a recent repeatability study for the contour method [14]). The bar cross section is 51.1 mm thick and 76.1 mm wide, with a length of 305 mm. The material properties for the bar are: E = 71 GPa, $\nu = 0.33$, with a yield strength of 490 MPa. The bar had residual stresses induced by heat treating to a T74 temper [15], which consisted of solution heat treatment at 477 °C for 3 h, immersion quenching in room temperature water with 16 % polyalkylene glycol (Aqua-Quench 260), and a dual artificial age at 121 °C for 8 h then 177 °C for 8 h. Based on earlier work, this treatment is expected to produce compressive residual stress on the bar exterior and tensile residual stress on the bar interior, both having magnitudes greater than 100 MPa [14, 16]. Contour method measurements were performed at the mid-length of the bar, as can be seen in Fig. 37.2.

The second contour method measurement was made in a long 316L stainless steel plate with an eight-pass groove weld of 308L stainless steel. The plate was the result of a concerted effort to design a sample to obtain data on the precision of residual stress measurements as described in [17]. The plate has a width of 152.4 mm (6 in.), height of 25.4 mm (1 in.), and a length of 1.22 m (48 in.) (Fig. 37.3a) with a groove along the plate length. The machined groove has a root width of 12.7 mm (0.5 in.), root depth of 6.35 mm (0.25 in.), and a wall angle of 70° (Fig. 37.3b). The material properties for the 316L stainless steel parent plate are: E = 206 GPa, $\nu = 0.3$, with a yield strength of 440 MPa, and the material properties for the 308L stainless steel weld filler metal are: E = 204 GPa, $\nu = 0.3$, with a yield strength of 350 MPa. The weld is made with machine controlled inert gas tungsten arc welding (GTAW). The details of the welding procedure can be found elsewhere [17]. A contour method measurement were performed at the mid-length of the plate at $z = 0$ (609.6 mm from each end), as can be seen in Fig. 37.3a.

A brief summary of the experimental steps of the contour method and its application for the two measurements will be given. Each sample was cut at the earlier described measurement plane using a wire electric discharge machine (EDM), while securely clamped. For each sample, the two resulting deformed cut surfaces were measured with a laser scanning profilometer along the cross-section with a measurement spacing of roughly 200 μm in both directions. The two surface profiles were then averaged on a common grid, and the average was fit to a smooth bivariate analytical surface. Residual stress on the contour plane was found by applying the negative of the smoothed surface profile as a displacement boundary

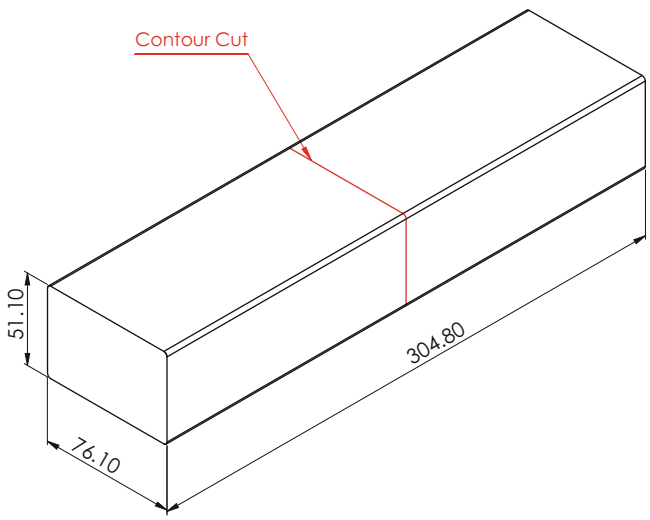

Fig. 37.2 Diagram of aluminum block and contour measurement location. Dimensions are in mm

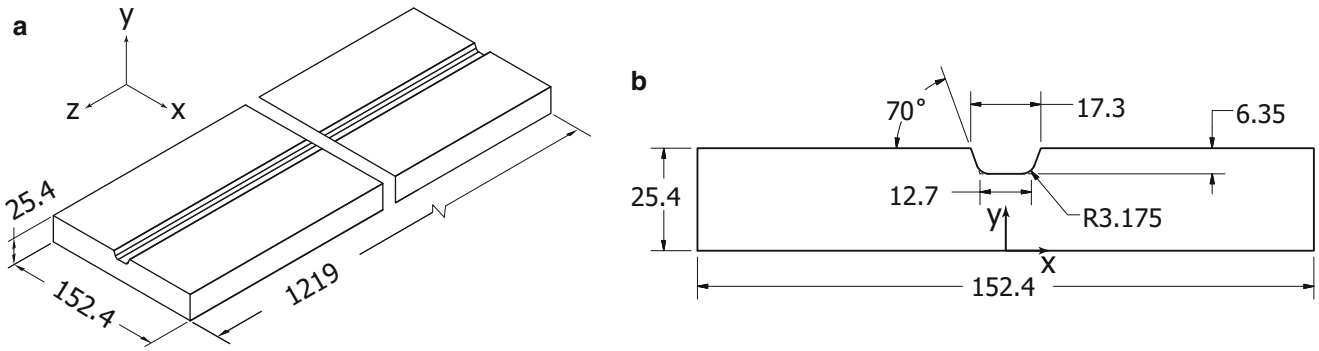

Fig. 37.3 Diagram of stainless steel weld plate (**a**) overall geometry and (**b**) cross-section with details of the machined groove. Dimensions are in mm

condition in a linearly elastic finite element (FE) model of the half plate. The FE analysis used commercial software [18], and a mesh of eight-node linear interpolation brick elements, with node spacing of roughly 1 mm on the cross-section in both directions, and biased node spacing in the out-of-plane direction.

37.3 Results

The results using the quenched aluminum bar can be seen in Fig. 37.4. The measured residual stress is shown in Fig. 37.4a. The contour method results are typical of a quenched aluminum component with compressive residual stress around the perimeter (−175 MPa) and tensile residual stress in the center (160 MPa). The calculated displacement error can be seen in Fig. 37.4b. The displacement error is very low at all points, but is slightly higher at the perimeter of the cross-section (around 2 MPa) than it is in the interior (around 1 MPa). The model error results can be seen in Fig. 37.4c. The results show that the model error is significantly higher at the perimeter of the cross-section (around 40 MPa) than in the interior (under 10 MPa at most locations). The total uncertainty estimate is shown in Fig. 37.4d.

Line plots of the of the measured residual stress with the total uncertainty estimate are shown as error bars in Fig. 37.5 for the quenched aluminum bar (labeled as Cut 1). These plots show the total uncertainty is relatively small compared to the range of the measured stress. Line plots of the displacement error, model error, and total uncertainty estimate are shown in Fig. 37.6 for the quenched aluminum bar. The results show that displacement error is very small compared to the model error, and in this case negligibly contributes to the total uncertainty estimate. The model error is under 10 MPa at most locations in the part interior, but is significantly higher at the perimeter of the cross section at a three localized areas toward the center of the bar.

The results for the stainless steel welded plate can be seen in Fig. 37.7. The measured residual stress is shown in Fig. 37.7a. The results show high tensile stress in the weld region, with a maximum near 450 MPa, giving way to nearby low magnitude compressive stresses (around −100 MPa), which is typical weld residual stress [19–21]. However, the results also show an area of larger compressive stress (about −250 MPa) toward the transverse edges, which was not expected, and may have been introduced during plate manufacture, prior to welding. The calculated displacement error can be seen in Fig. 37.7b. The displacement error is low at all points, but is slightly higher at the perimeter of the cross-section (some points as high as 10 MPa) than it is in the interior (around 2 MPa). The model error results can be seen in Fig. 37.7c. The results show that the model error is significantly higher at the perimeter of the cross-section (around 100 MPa) than in the interior (under 30 MPa at most locations). The total uncertainty estimate is shown in Fig. 37.7d, which has essentially the same distribution as the model error, but with the low uncertainty being replaced with a floor.

Line plots of the of the measured residual stress with the total uncertainty estimate are shown as error bars in Fig. 37.8 for the stainless steel welded plate (labeled as Cut 1). These plots show the total uncertainty is a significant percentage of the measured stress range. Line plots of the displacement error, model error, and total uncertainty estimate are shown in Fig. 37.9 for the stainless steel welded plate. The results show that displacement error is very small compared to the model error, and in this case negligibly contributes to the total uncertainty estimate. The model error is under 30 MPa at most locations in the part interior, but is significantly higher at the perimeter of the cross section which causes the mean of the uncertainty to be high (46 MPa), and thus dominates the total uncertainty distribution.

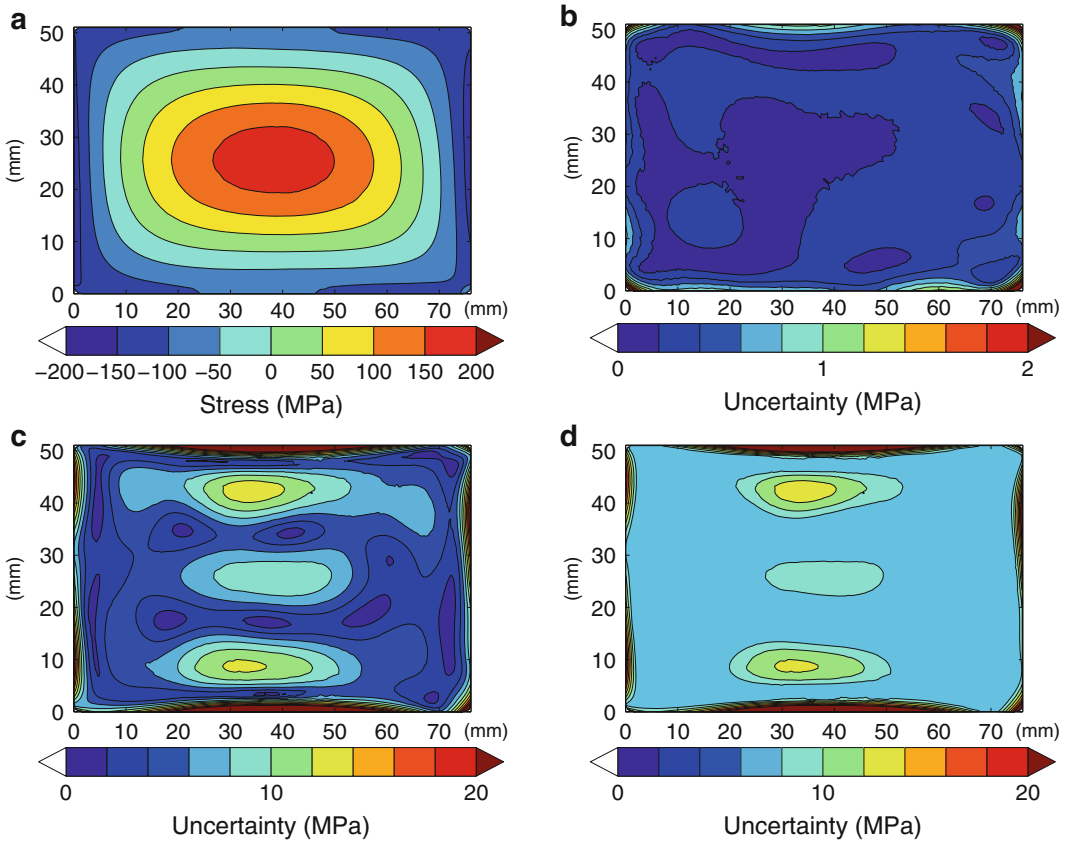

Fig. 37.4 Results from the contour method measurement in a quenched aluminum bar: (**a**) measured residual stress, (**b**) displacement error, (**c**) model error, and (**d**) total uncertainty

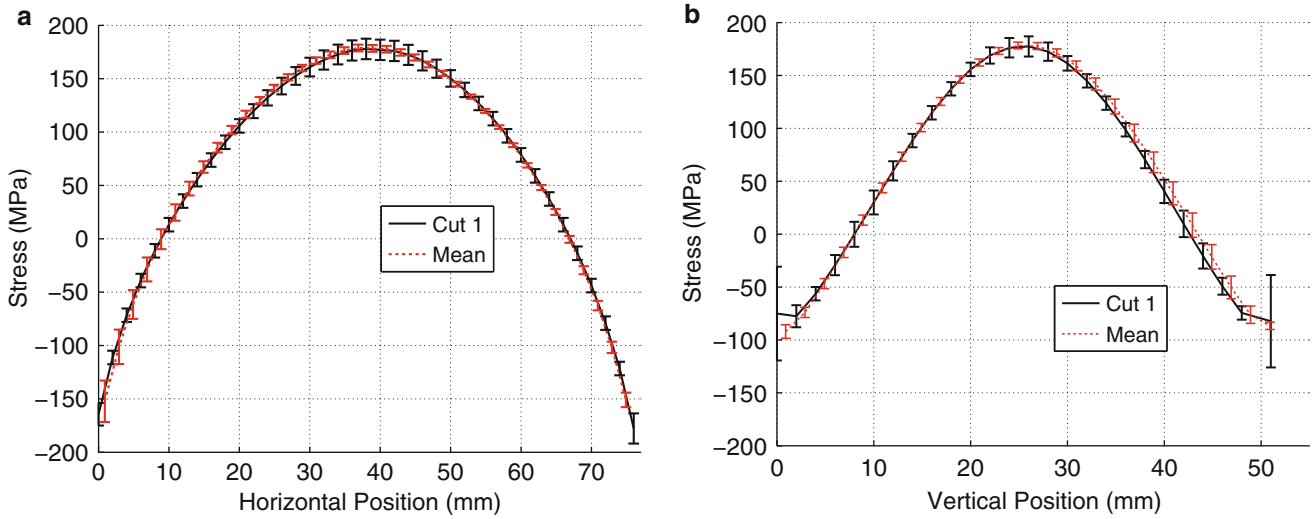

Fig. 37.5 Line plots of the measured residual stress in the quenched aluminum bar with the total uncertainty shown as error bars along the (**a**) horizontal direction at the mid-thickness (y = 25.4 mm) and (**b**) vertical direction at the mid-width (x = 38.1 mm)

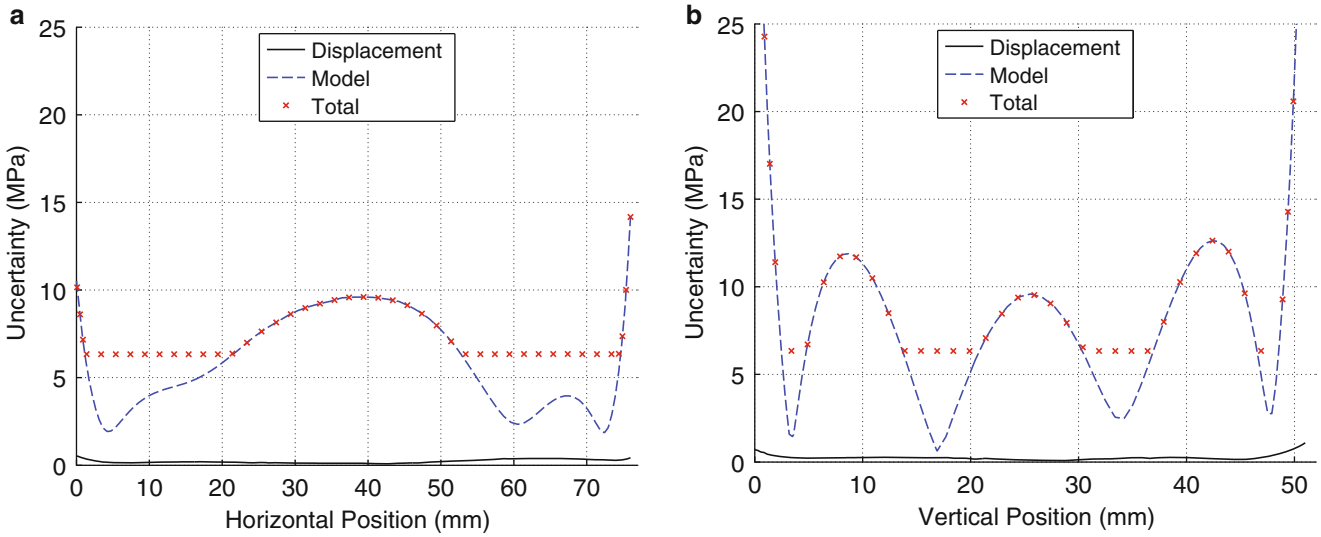

Fig. 37.6 Line plots of the displacement error, model error, and total uncertainty in the quenched aluminum bar along the (**a**) horizontal direction at the mid-thickness (y = 25.4 mm) and (**b**) vertical direction at the mid-width (x = 38.1 mm)

37.4 Discussion

The nominally small model error in both samples indicates that the smoothing tends to be robust in the part interior, whereas the smoothing is less stable at the part boundary, which is indicated by the larger uncertainties at the boundary.

The uncertainty is significantly larger in the stainless steel welded plate. There appears to be two reasons for that. One, as suggested in [10], the uncertainty does appear to scale with the elastic modulus. For a given amount of residual stress, a sample with a larger elastic modulus will exhibit a lower displacement, which is measured experimentally. The second reason for the larger uncertainty in the stainless steel welded plate is due to the more complicated stress field that is being measured, and as a result is more difficult to fit with a finite number of coefficients in the analytical surface.

Both of the measurements presented here were used in repeatability studies of the contour method. Repeatability studies are especially useful to compare with this study because they offer an alternative method to calculate uncertainty (assuming each measurement has the same underlying stress). The mean of the measurement population and the repeatability standard deviation can be seen in the line plots in Fig. 37.5 for the quenched aluminum bar. Comparing an individual measurement from that data set and its estimated uncertainty (Cut 1) to the mean of the measurement set and its repeatability standard deviation shows that the uncertainty estimate is reasonable. The two lines have error bars that overlap at all points, indicating that there is no statistical difference between the two lines with their associated uncertainties. Further details regarding the repeatability study in the quenched aluminum bars can be found in [10]. We find similar results when looking at the results for one measurement in the stainless steel welded plate compared with mean of a set of repeated measurements, as is shown in Fig. 37.8. As was found in the quenched aluminum bar results, the results for the stainless steel welded plate have error bars that overlap both lines at all points, indicating that there is no statistical difference between the two lines with their associated uncertainties. Further details regarding the repeatability study in the stainless steel welded plate can be found in [17].

Overall, the uncertainty estimates in both cases appear to be reasonable and give much needed uncertainty estimates for a single contour method measurement.

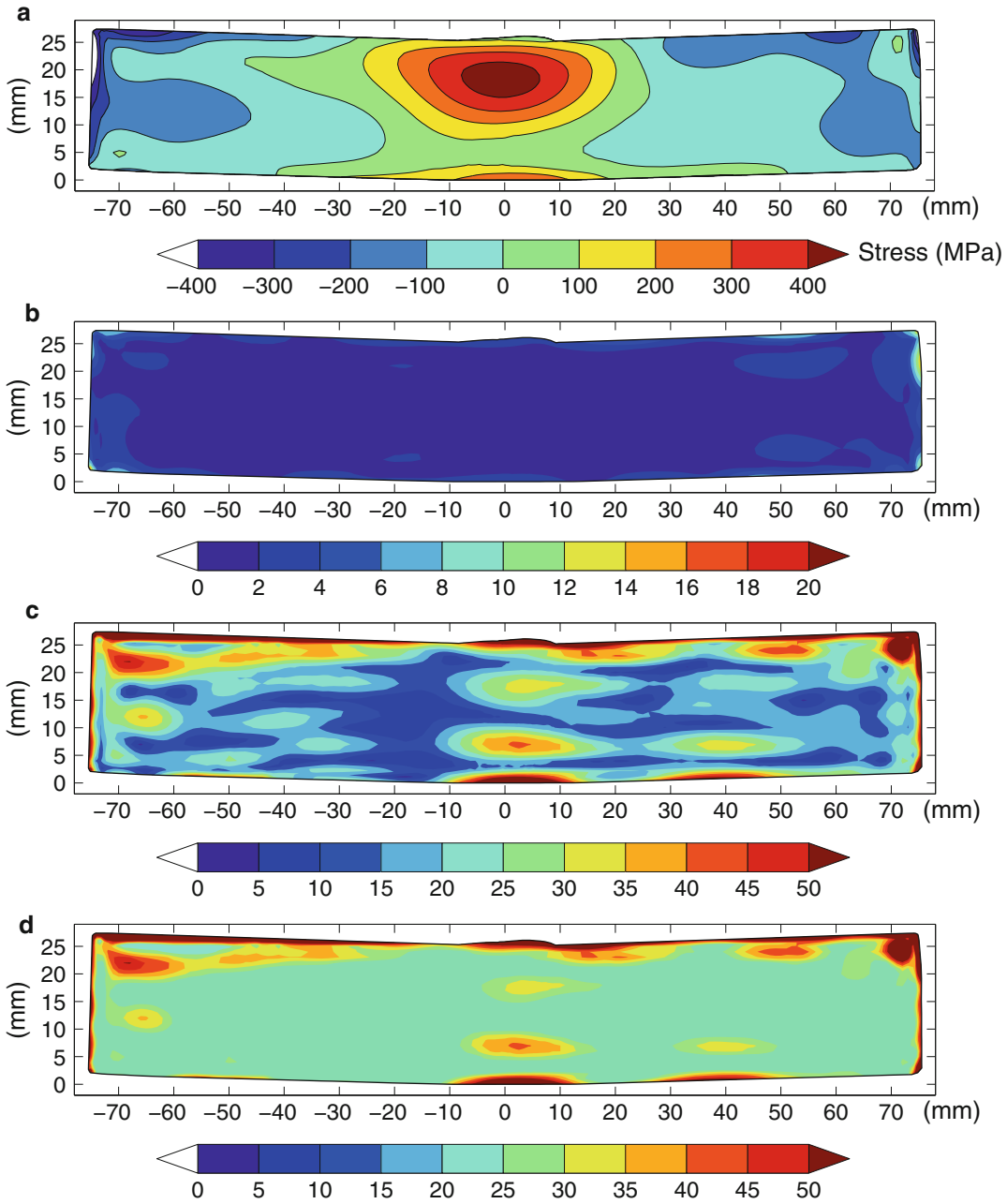

Fig. 37.7 Results from the contour method measurement in a stainless steel welded plate: (**a**) measured residual stress, (**b**) displacement error, (**c**) model error, and (**d**) total uncertainty

37.5 Summary/Conclusions

This paper describes a single measurement uncertainty estimator for the contour method, which accounts for noise in measured displacement field and error associated with smoothing. This represents a significant improvement over available techniques for contour method uncertainty estimation. The error arising from noise in the measured displacement field is estimated using a Monte Carlo approach by finding the standard deviation of the differences in stress resulting from applying normally distributed noise to the measured surface. The error associated with the smoothing model for the displacement field was found by taking the standard deviation of stresses computed using different levels of smoothing.

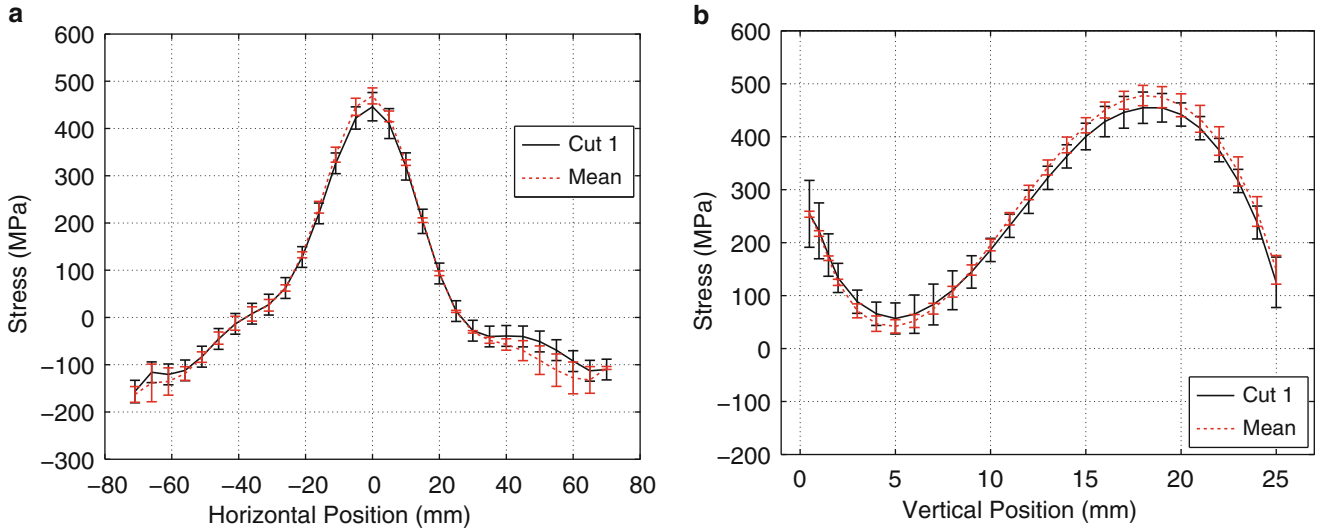

Fig. 37.8 Line plots of the measured residual stress in the stainless steel welded plate with the total uncertainty shown as error bars along the (**a**) horizontal direction at the weld root (y = 17 mm) and (**b**) vertical direction at the mid-width (x = 0)

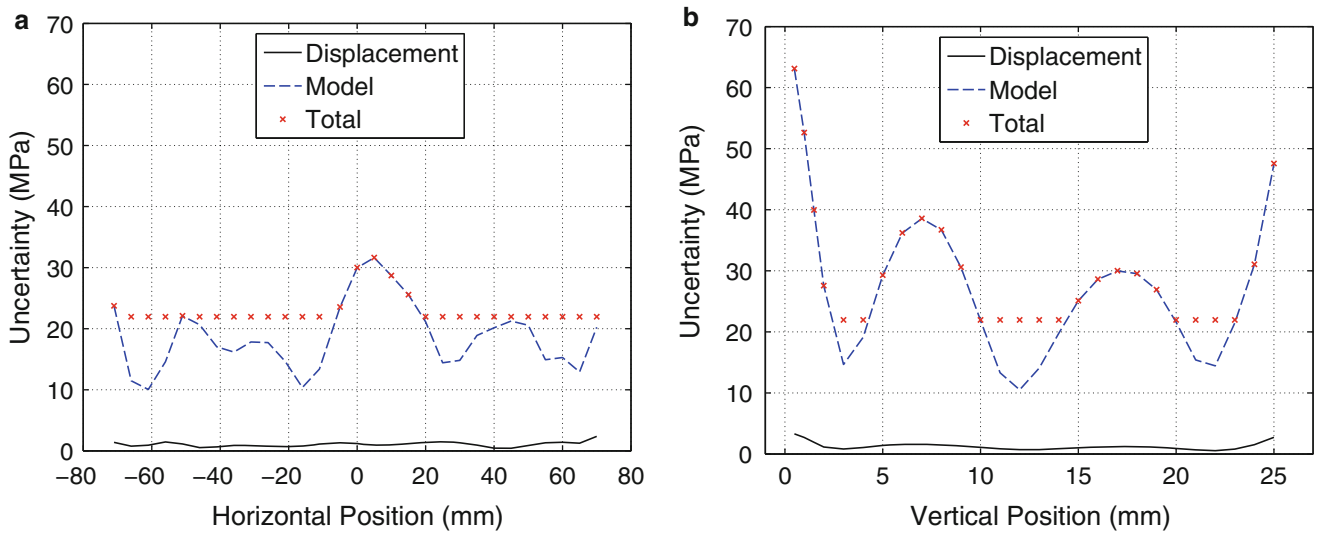

Fig. 37.9 Line plots of the displacement error, model error, and total uncertainty in the stainless steel welded plate along the (**a**) horizontal direction at the weld root (y = 17 mm) and (**b**) vertical direction at the mid-width (x = 0)

The uncertainty estimate was evaluated in two contour method experiments. The uncertainty estimates have similar features for both samples, including: very low displacement error (appears to be negligible in the two cases examined), low model error in the interior, higher model error along the part perimeter, and the total uncertainty distribution is dominated by the model error. The uncertainty in the stainless steel sample is systemically higher than that found in the aluminum sample.

Acknowledgements With gratitude, the authors acknowledge the U.S. Air Force Research Laboratory for providing financial support for this work (contract FA8650-14-C-5026). The authors would also like to acknowledge helpful discussions with David Riha and John McFarland from the Southwest Research Institute related to uncertainty quantification.

References

1. M.B. Prime, Cross-sectional mapping of residual stresses by measuring the surface contour after a cut. J. Eng. Mater. Technol. **123**, 162–168 (2001)
2. J. Kelleher, M.B. Prime, D. Buttle, P.M. Mummery, P.J. Webster, J. Shackleton et al., The measurement of residual stress in railway rails by diffraction and other methods. J Neutron Res **11**, 187–193 (2003)
3. D.W. Brown, T.M. Holden, B. Clausen, M.B. Prime, T.A. Sisneros, H. Swenson et al., Critical comparison of two independent measurements of residual stress in an electron-beam welded uranium cylinder: neutron diffraction and the contour method. Acta Mater. **59**, 864–873 (2011)
4. M.B. Prime, A.T. DeWald, *Practical Residual Stress Measurement Methods (Ch. 5)* (Wiley, West Sussex, 2013)
5. A.T. DeWald, J.E. Rankin, M.R. Hill, M.J. Lee, H.-L. Chen, Assessment of tensile residual stress mitigation in Alloy 22 welds due to laser peening. J. Eng. Mater. Technol. **126**, 465–473 (2004)
6. F. Hosseinzadeh, P. Ledgard, P.J. Bouchard, Controlling the cut in contour residual stress measurements of electron beam welded Ti-6Al-4V alloy plates. Exp. Mech. **53**, 829–839 (2012)
7. M.B. Prime, T. Gnäupel-Herold, J.A. Baumann, R.J. Lederich, D.M. Bowden, R.J. Sebring, Residual stress measurements in a thick, dissimilar aluminum-alloy friction stir weld. Acta Mater. **54**, 4013–4021 (2006)
8. F. Hosseinzadeh, P.J. Bouchard, Mapping multiple components of the residual stress tensor in a large P91 steel pipe girth weld using a single contour cut. Exp. Mech. **53**, 171–181 (2012)
9. M.B. Prime, R.J. Sebring, J.M. Edwards, D.J. Hughes, P.J. Webster, Laser surface-contouring and spline data-smoothing for residual stress measurement. Exp. Mech. **44**, 176–184 (2004)
10. M.D. Olson, A.T. DeWald, M.R. Hill, M.B. Prime, Estimation of uncertainty for contour method residual stress measurements. Exp. Mech. **55**, 577–585 (2014)
11. M.B. Prime, M.R. Hill, Uncertainty, model error, and order selection for series-expanded, residual-stress inverse solutions. J. Eng. Mater. Technol. **128**, 175 (2006)
12. H.W. Coleman, W.G. Steele, *Experimentation, Validation, and Uncertainty Analysis for Engineers (Ch. 2)* (Wiley, Hoboken, 2009)
13. J.M. Hammersley, D.C. Handscomb, *Monte Carlo Methods* (Halsted Press, Sydney, 1964)
14. M.R. Hill, M.D. Olson, Repeatability of the contour method for residual stress measurement. Exp. Mech. **54**, 1269–1277 (2014)
15. SAE Aerospace, Heat Treatment of Wrought Aluminum Alloy Parts, AMS 2770, 2006
16. J.S. Robinson, D.A. Tanner, C.E. Truman, A.M. Paradowska, R.C. Wimpory, The influence of quench sensitivity on residual stresses in the aluminium alloys 7010 and 7075. Mater. Charact. **65**, 73–85 (2012)
17. M.D. Olson, M.R. Hill, E. Willis, A.G. Peterson, V.I. Patel, O. Muránsky, Assessment of weld residual stress measurement precision: mock-up design and results for the contour method. J. Nuclear Eng. Rad. Sci. **1**, 031008 (10 pages) (2015)
18. Abaqus/Standard, Version 6.10, Providence, RI, 2010
19. C. Ohms, R.C. Wimpory, D.E. Katsareas, A.G. Youtsos, NET TG1: residual stress assessment by neutron diffraction and finite element modeling on a single bead weld on a steel plate. Int. J. Press. Vessel. Pip. **86**, 63–72 (2009)
20. M.C. Smith, A.C. Smith, NeT bead-on-plate round robin: comparison of residual stress predictions and measurements. Int. J. Press. Vessel. Pip. **86**, 79–95 (2009)
21. P.J. Bouchard, The NeT bead-on-plate benchmark for weld residual stress simulation. Int. J. Press. Vessel. Pip. **86**, 31–42 (2009)